Supplementary Fig. S1. Specificity of antibodies used to detect overexpressed hTERT. (a) Wild-type (WT) and variant 3xFLAG-hTERT proteins were overexpressed in HEK293T cells along with hTR. -, no hTERT plasmid. Western blot with the anti-hTERT antibody Abcam Ab32020 detects all variants except F1127L, which has a mutation in the epitope. (b) Same samples probed with the anti-FLAG antibody, confirming that the F1127L variant is expressed.

Supplementary Fig. S2. RRL assays performed independently by two different researchers, A and B. A, 3xFLAG-tagged hTERT. B, HA-tagged hTERT.

Supplementary Fig. S3. Reverting the mutant hTERTs to wild-type confirms that reduced activity is due to the indicated mutation. All hTERTs were assembled with WT hTR in RRLs.

Supplementary Fig. S4. Dependence of telomerase activity on the amount of plasmid DNA transfected in HEK cells. (a) and (b) Telomerase activity assays with equal numbers of cells transfected with different amounts of *hTERT* plasmid, always with 4 µg *hTR* plasmid. (c) and (d) Telomerase activity assays with equal numbers of cells transfected with different amounts of *hTR* plasmid, always with 1.0 µg *hTERT* plasmid. *Standard conditions used throughout this work.

Supplementary Fig. S5. Activity is linear with the amount of telomerase beads used in the assay, and Western analysis of hTERT protein shows how hTERT levels can be quantified using a standard curve. (a)Direct telomerase assays with different amounts of anti-FLAG telomerase beads. The standard condition for the assays in this work was 6 µL beads. (b) Quantification of panel a shows that the assay is in the linear range with respect to telomerase concentration. (c) FLAG-hTERT proteins containing various mutations were expressed in HEK cells (top) and hTERT levels were quantified using a standard curve (bottom).

Supplementary Fig. S6. Time dependence of telomerase activity. (a) HEK cell telomerase activity as a function of time, duplicate samples. Lanes M, markers for primer extended by 2 or 4 nt.
(b) Quantification of data in panel a. (c) Direct test of stability of telomerase enzyme by preincubation of telomerase at 30°C in assay buffer for various times prior to addition of nucleotides and 60-min reaction.
(d) Quantification of panel c, showing that enzyme activity decreases slowly as a function of incubation time.

Supplementary Fig. S7. Telomerase expressed in the VA13 ALT cell line gives similar activity as that expressed in HEK cells. (a) Western analysis of hTERT proteins using anti-FLAG antibody.
(b) Quadruplicate repeats of activity assays of hTERT alleles expressed with wild-type hTR in VA13 cells. Lanes M, markers for primer extended by 2 or 4 nt.

Supplementary Fig. S8. Justification for including the high molecular weight “smear” of telomerase products when quantifying telomerase activity. Our standard gel electrophoresis time is 1 hour 40 min. When the reaction products are subjected to electrophoresis for a longer time (3.5 and 5.0 hours), it becomes clear that the high molecular weight smear consists of discrete reaction products with the characteristic six-nucleotide repeat. M, markers consisting of double-stranded DNA restriction fragments allow identification of telomeric repeat number in cases where low molecular weight fragments have run off the gel.

Supplementary Fig. S9. Crystal structure (pdb entry 3KYL) of the *Tribolium* TERT complexed with an RNA-DNA template-primer pair [M. Mitchell, A. Gillis, M. Futahashi, H. Fujiwara & E. Skordalakes.

Structural basis for telomerase catalytic subunit TERT binding to RNA template and telomeric DNA. *Nat. Struc. Molec. Biol.* (2009).] Multiple sequence alignment was used to identify the *Tribolium* amino acids corresponding to those in hTERT. Two amino acids mutated in human disease are highlighted.

Supplementary Fig. S10. Prediction of activity of mutant telomerases by the PolyPhen-2 algorithm. Bar graph comparing R, the measured activity of the telomerase variants assembled in RRLs (this work), with P, the probability that the mutation will be benign as predicted by the PolyPhen-2 algorithm. Because the PolyPhen-2 score is the probability that the mutation will be damaging, 1 – PolyPhen Score is plotted to allow direct comparison with activity data.

Supplementary Figure S1

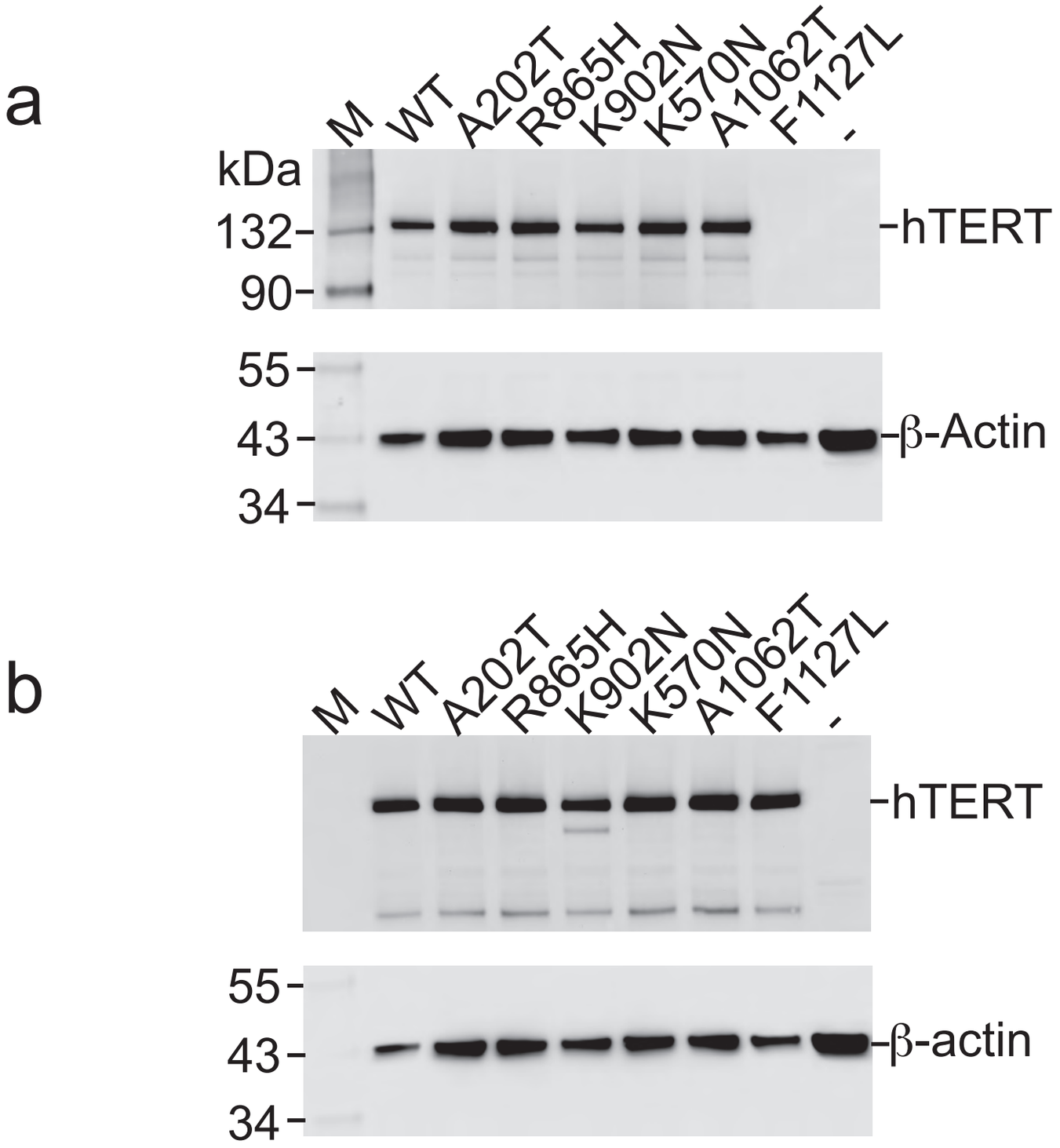

Supplementary Figure S2

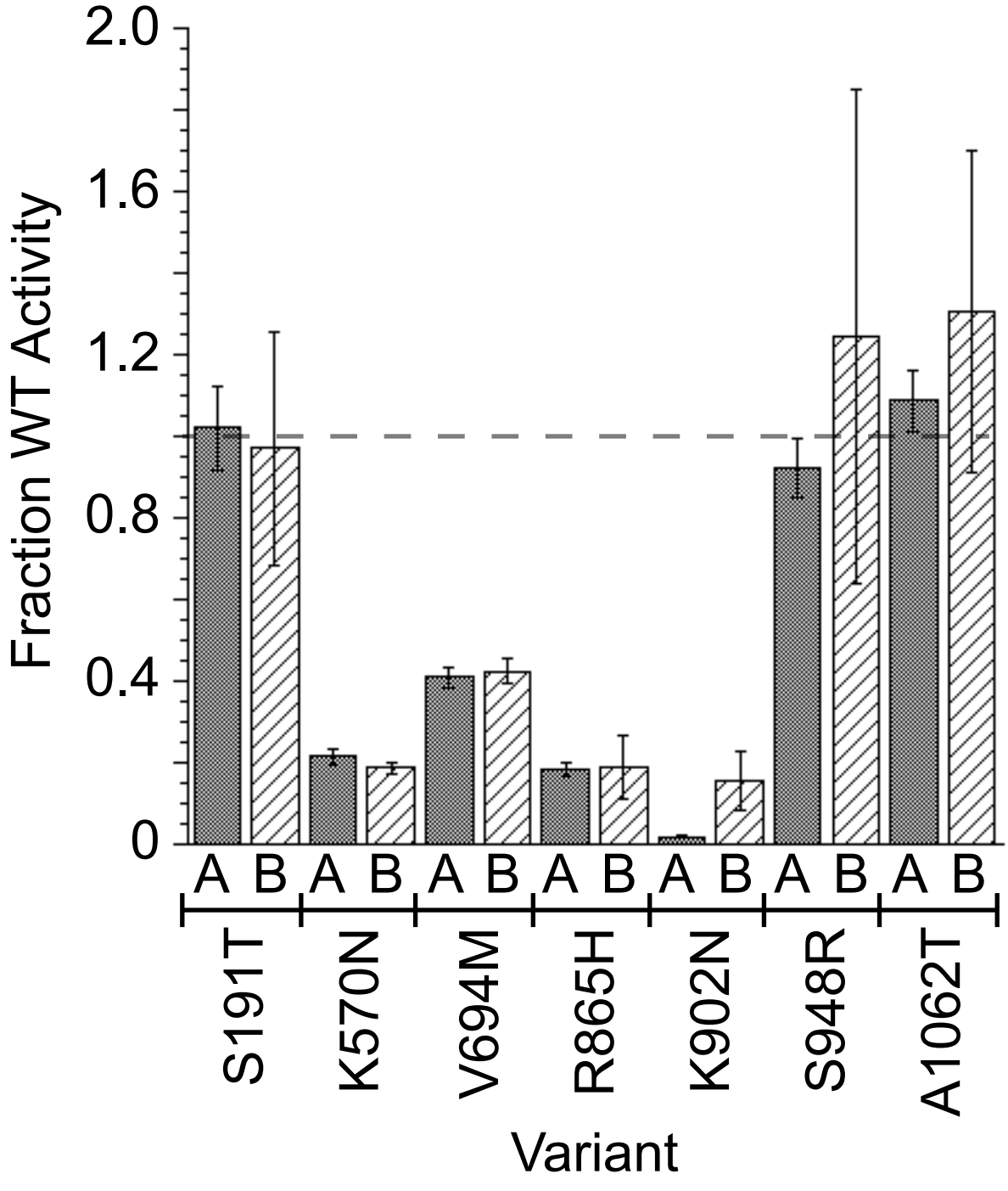

Supplementary Figure S3

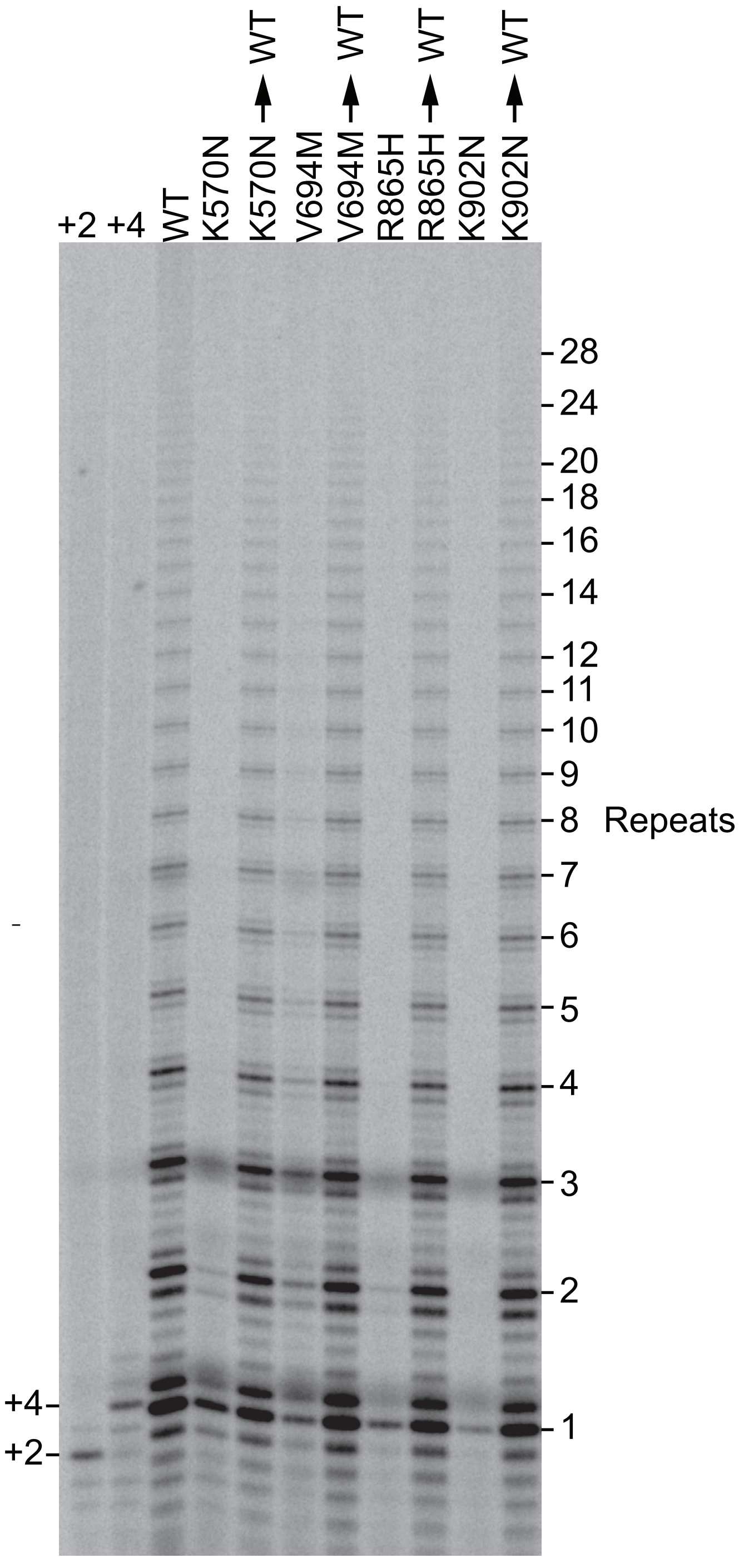

Supplementary Figure S4

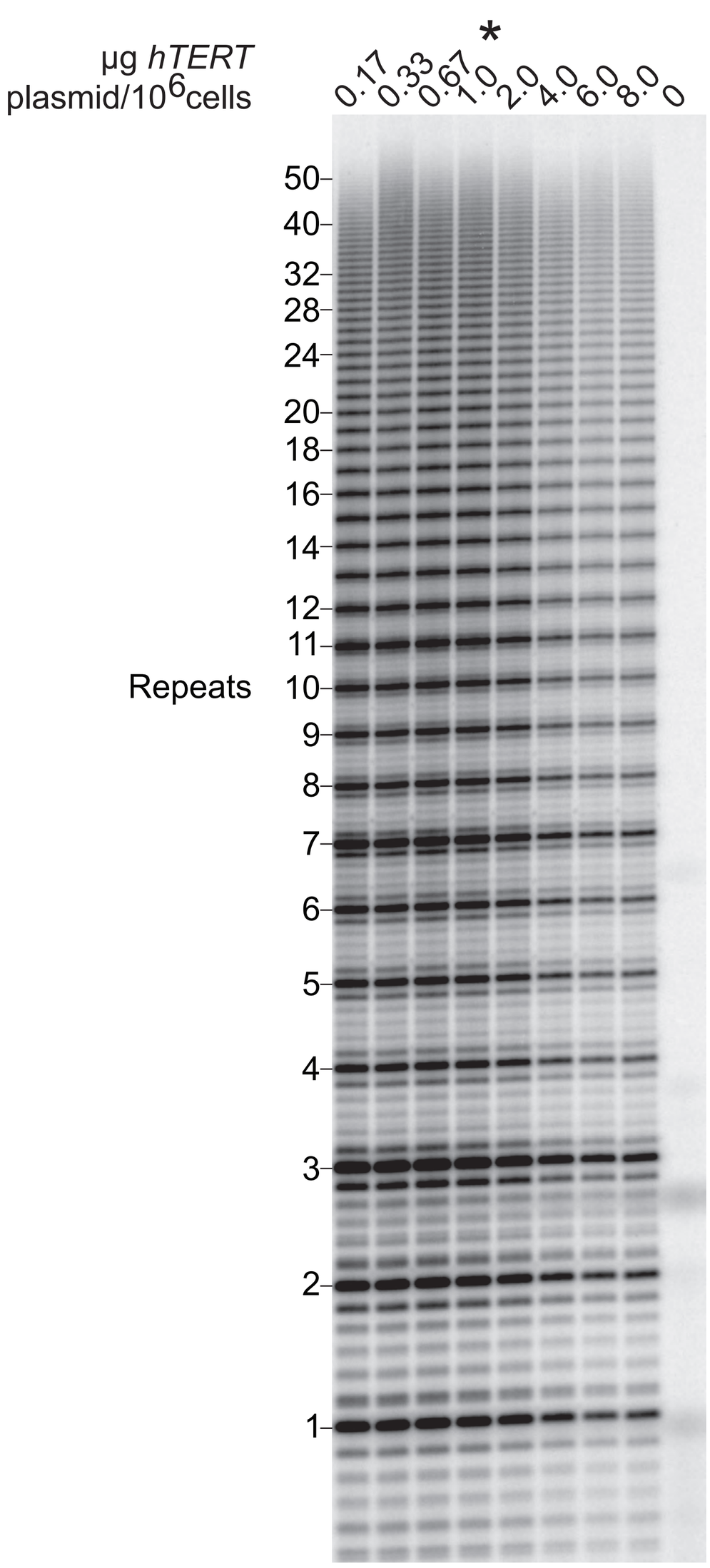

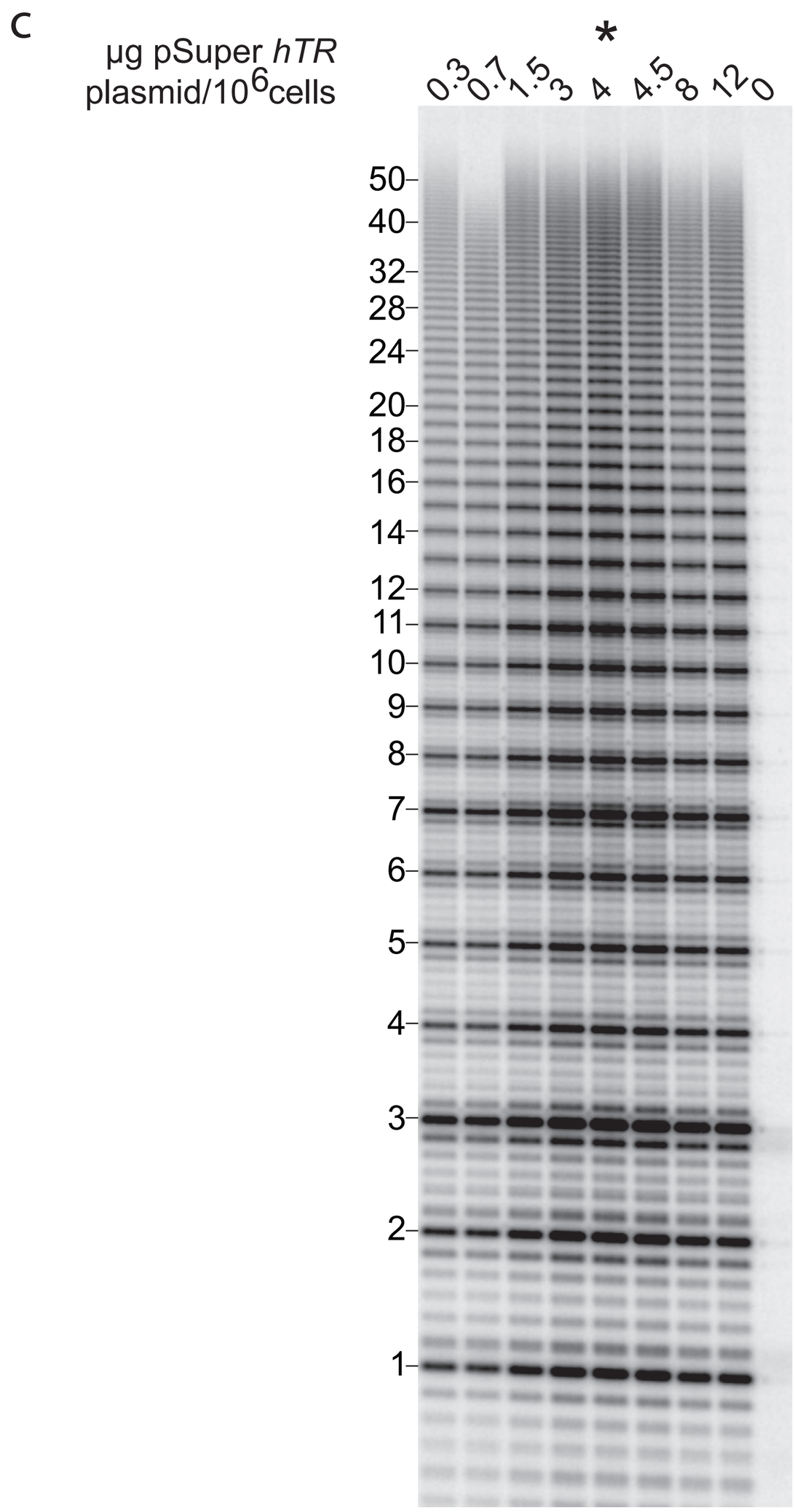

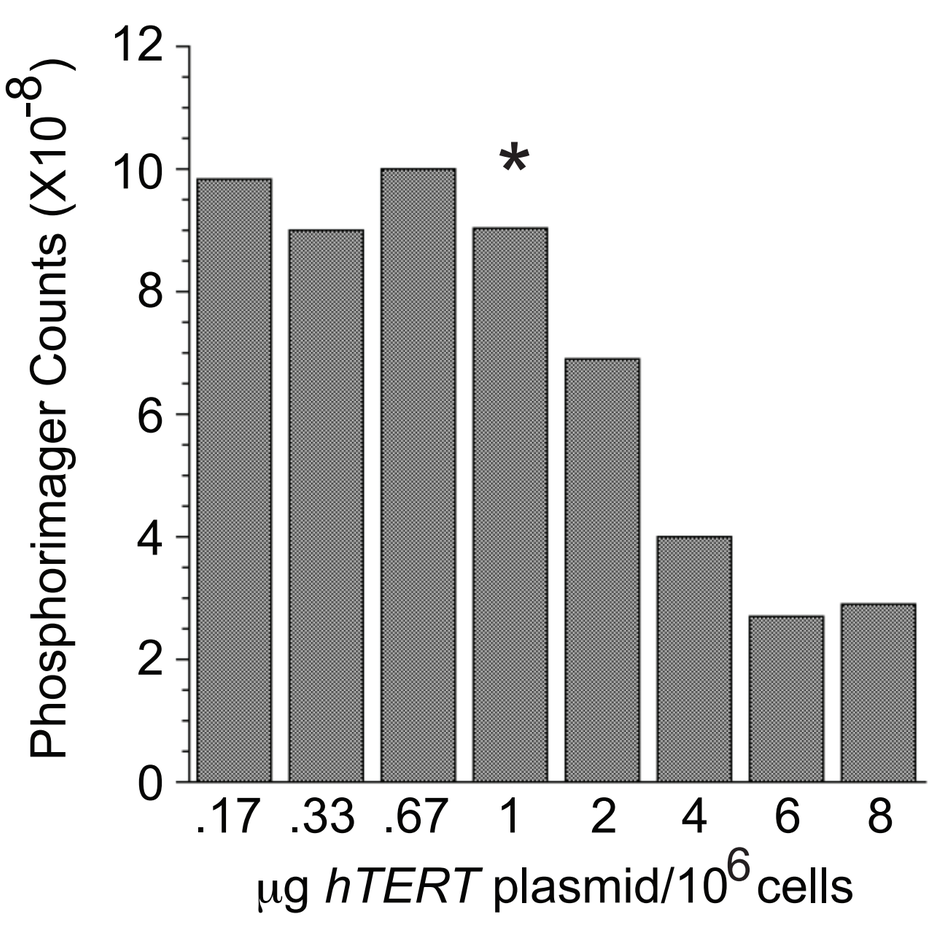

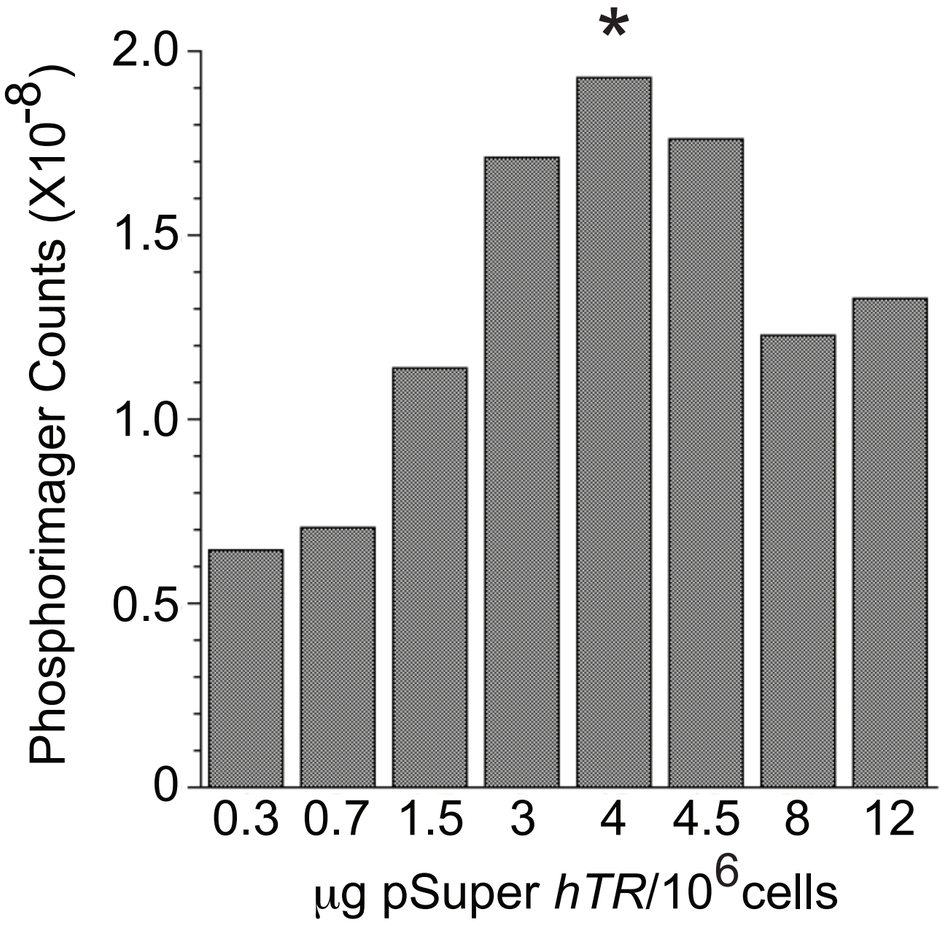

Supplementary Figure S5

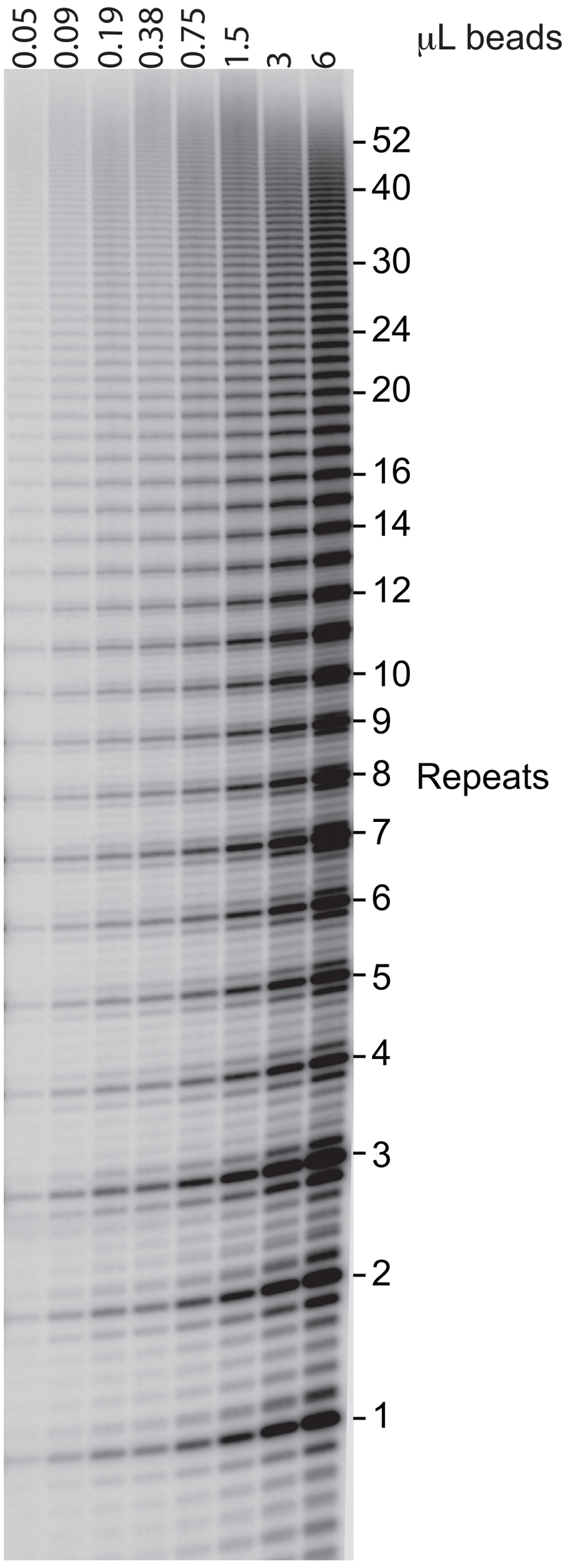

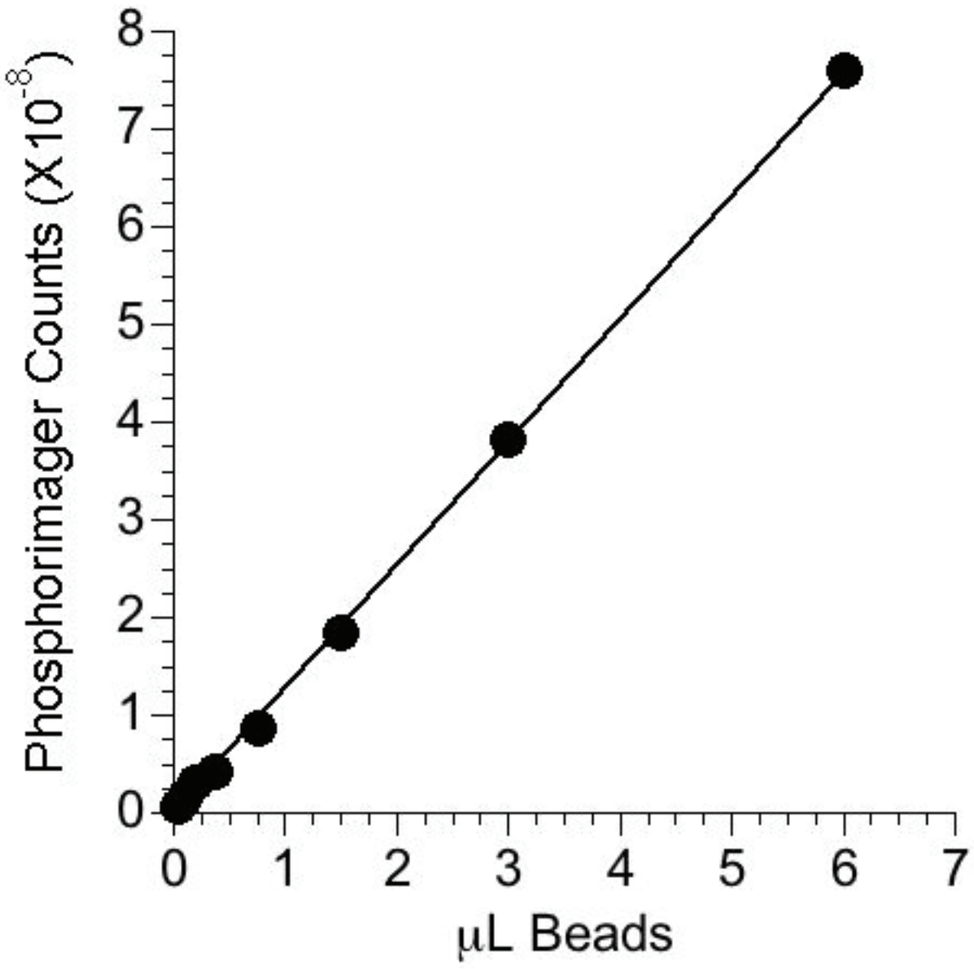

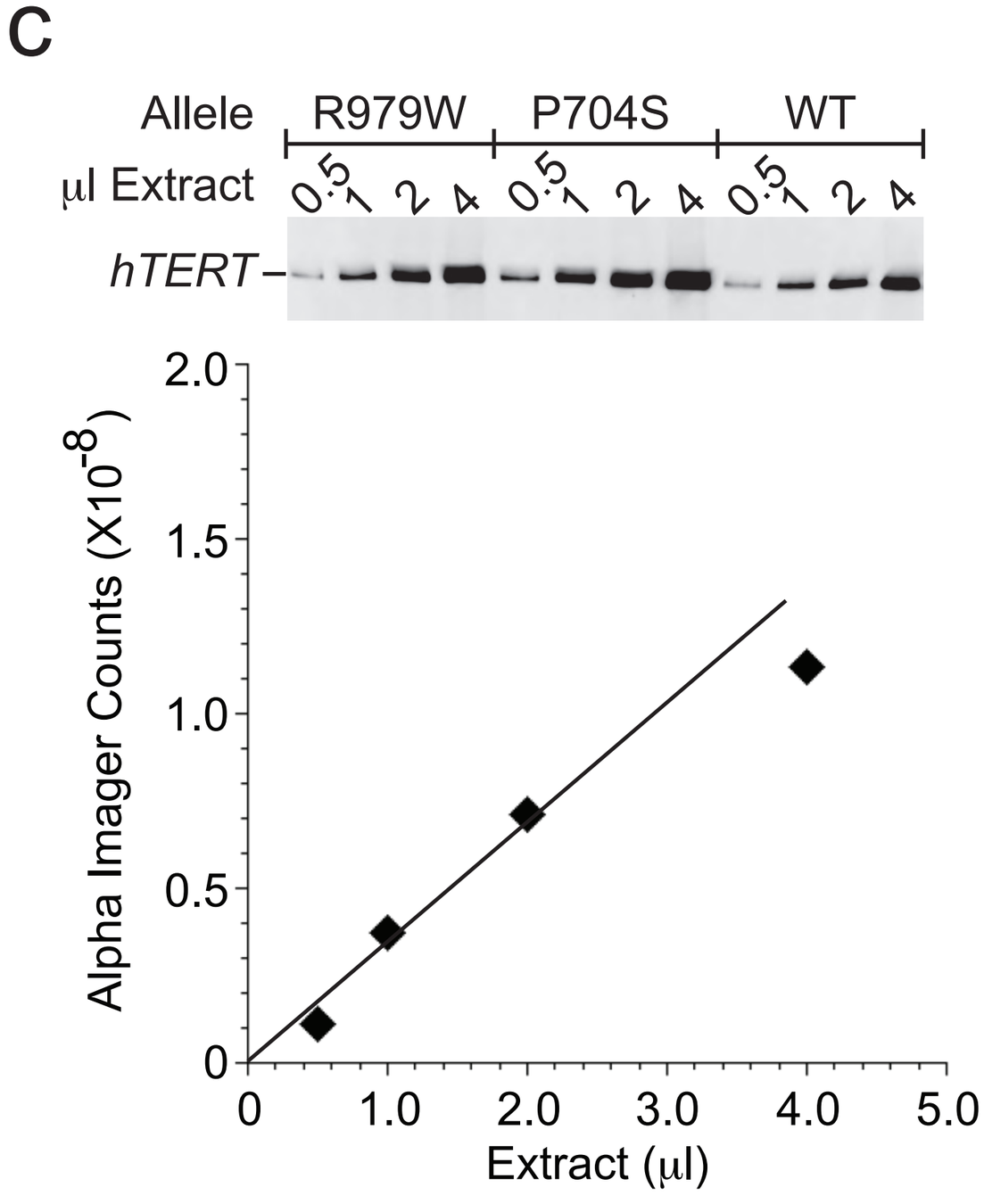

Supplementary Figure S6

a

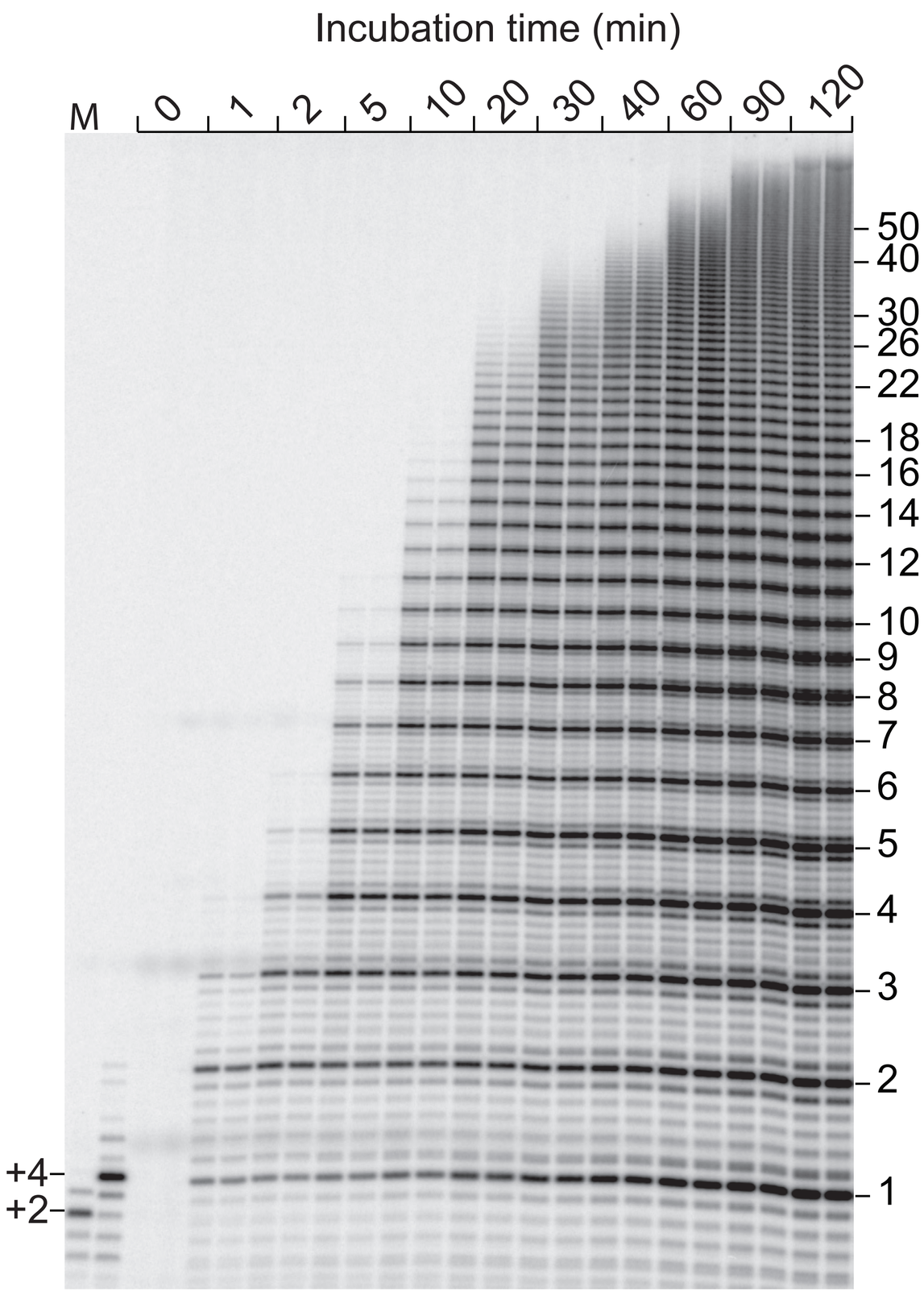

b

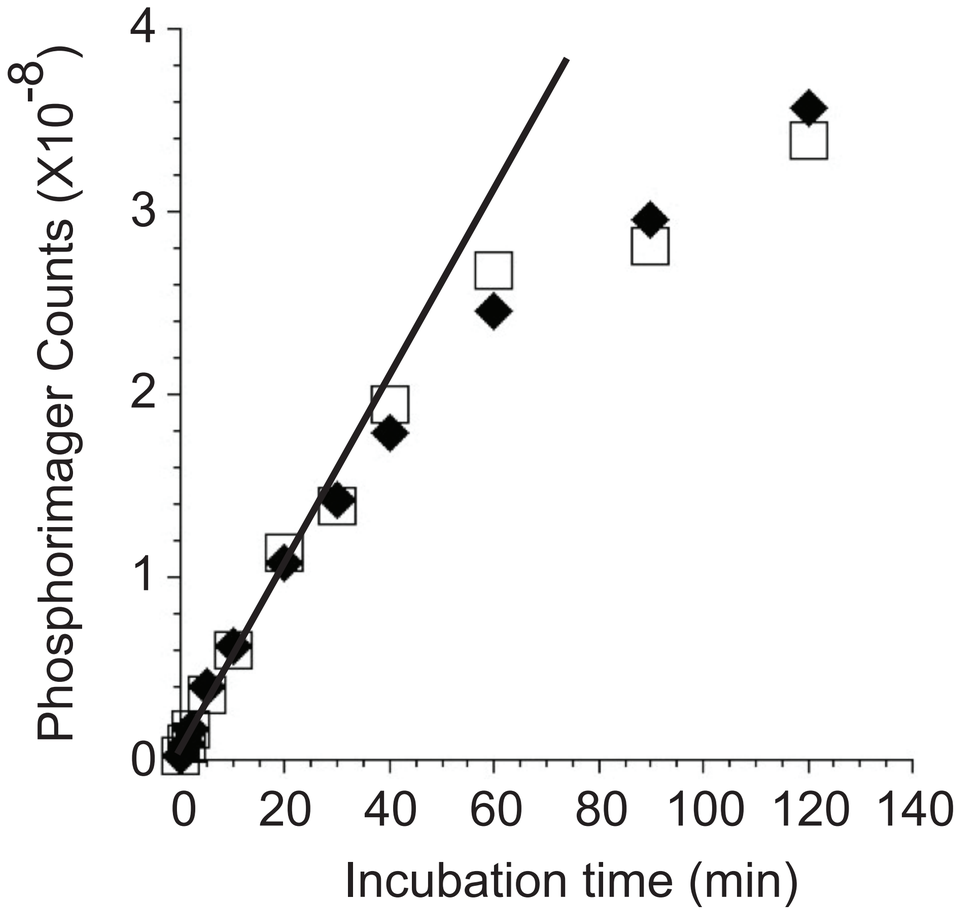

c

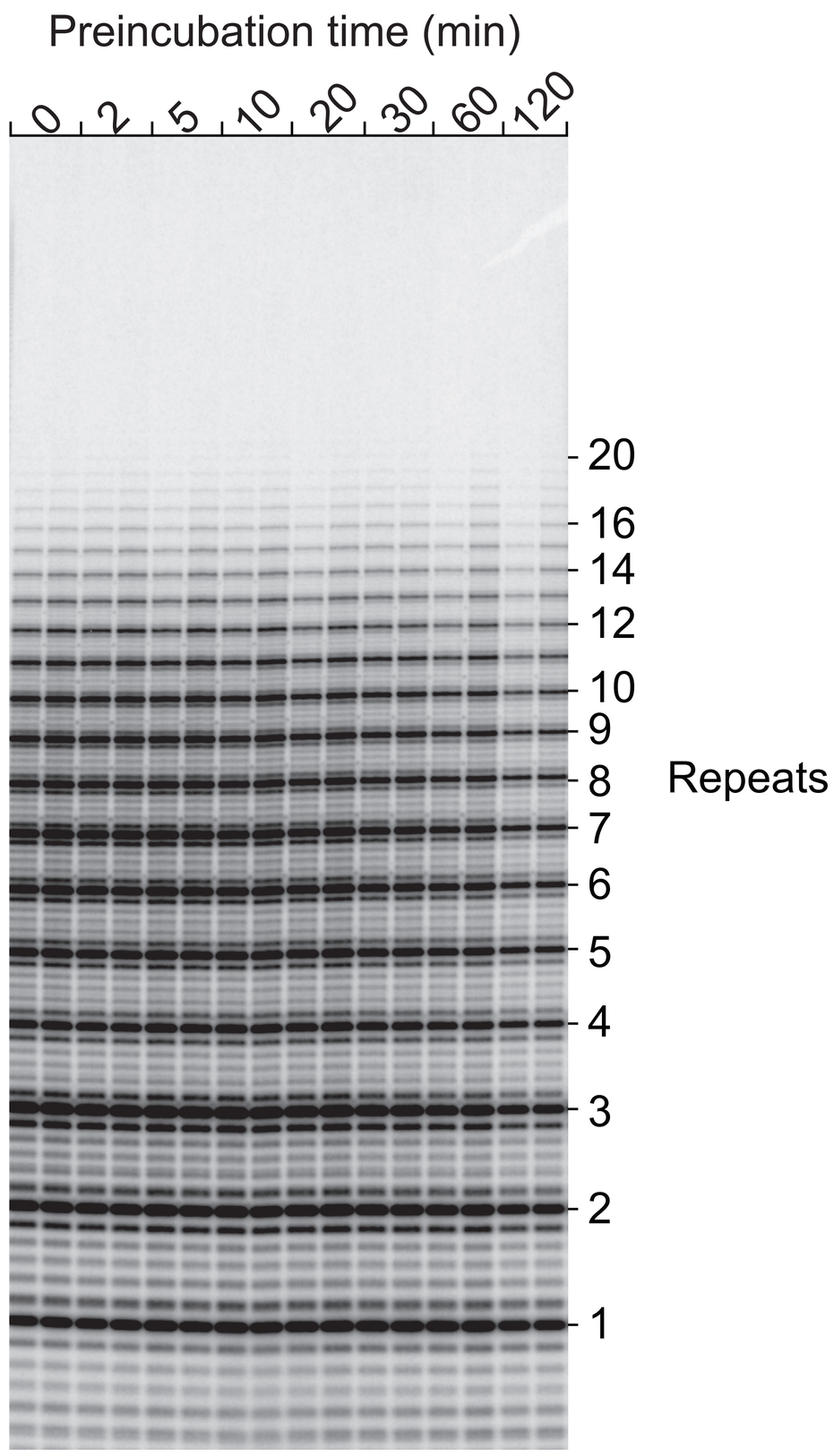

d

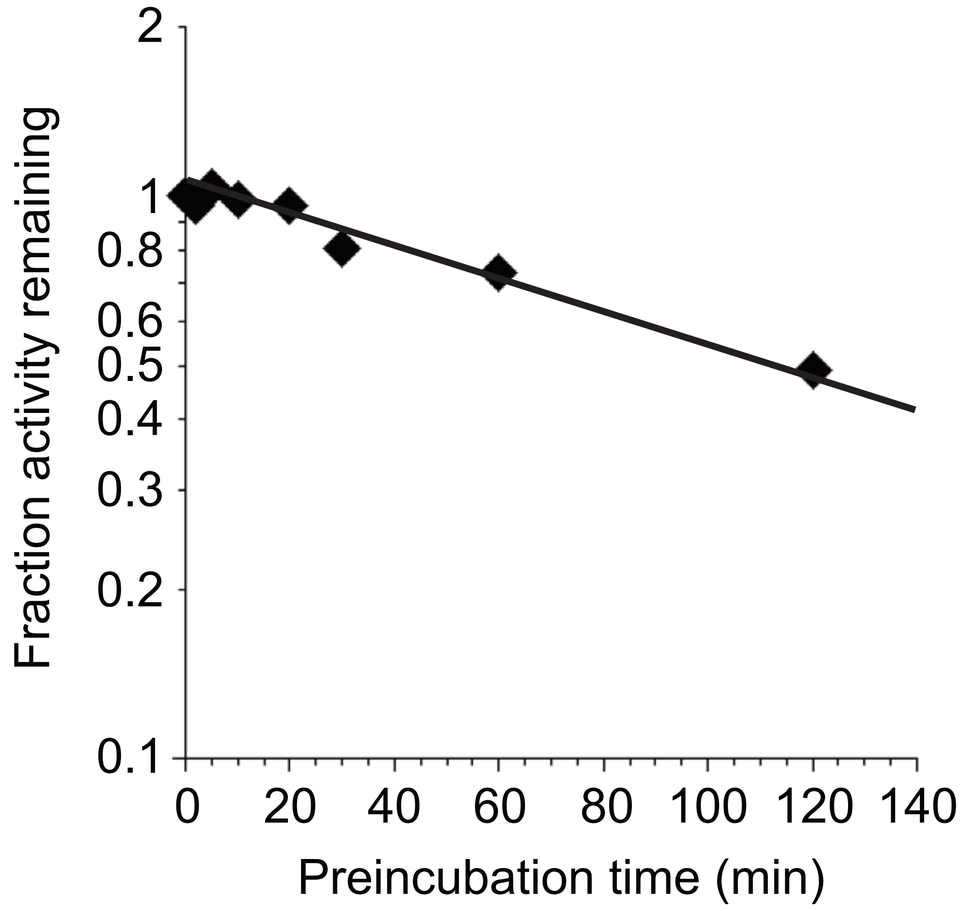

Supplementary Figure S7

a

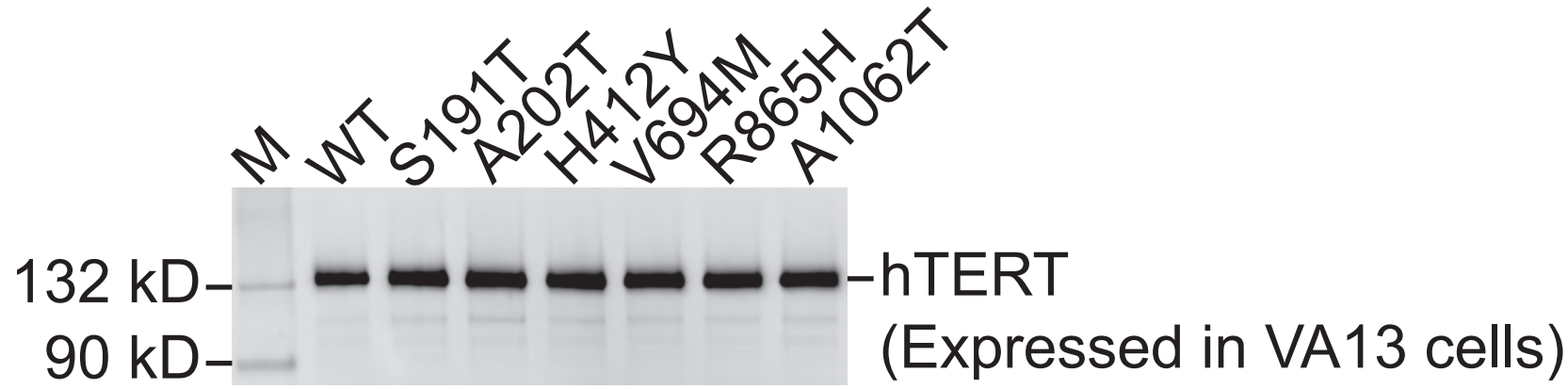

b

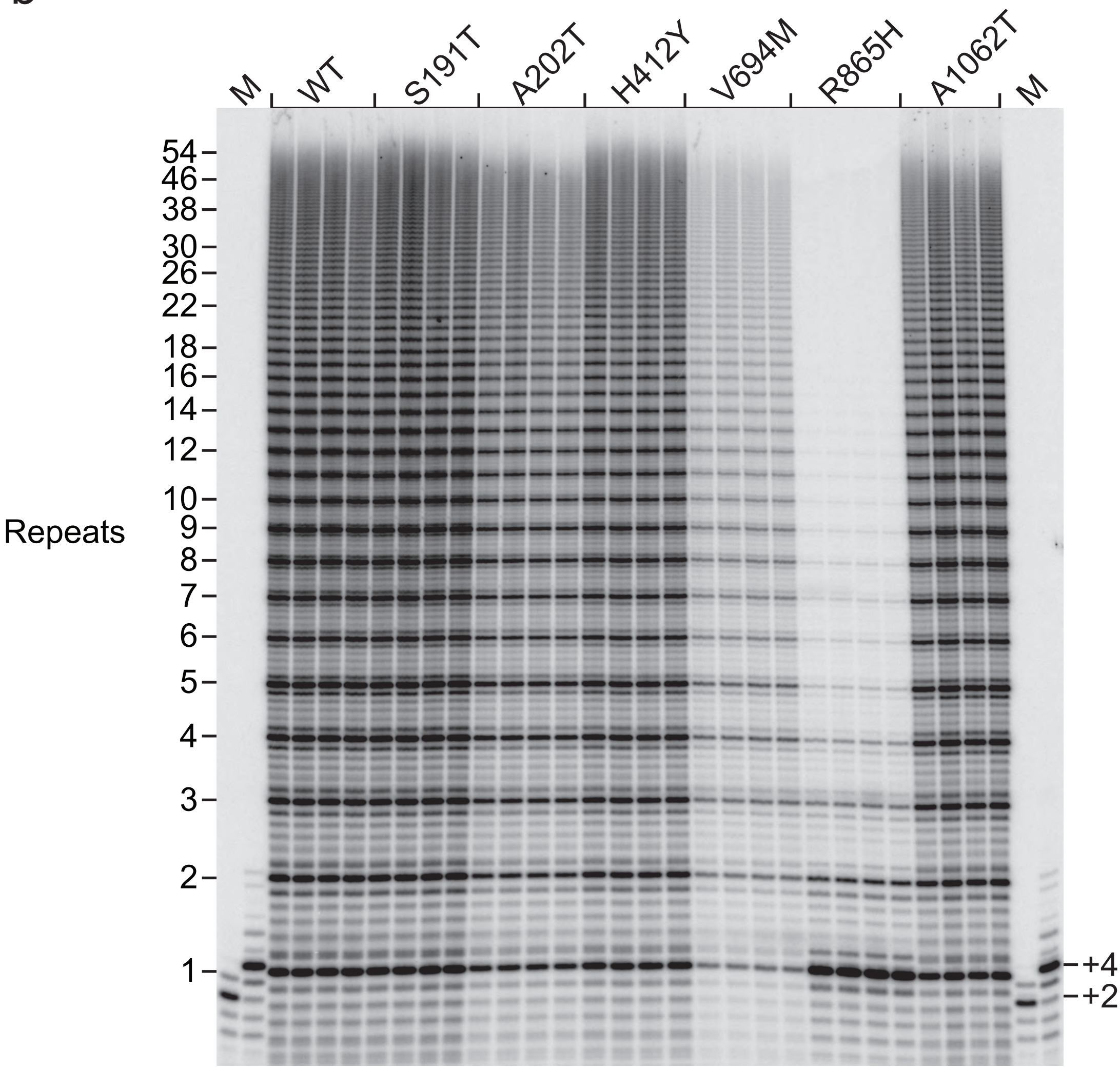

Supplementary Figure S8

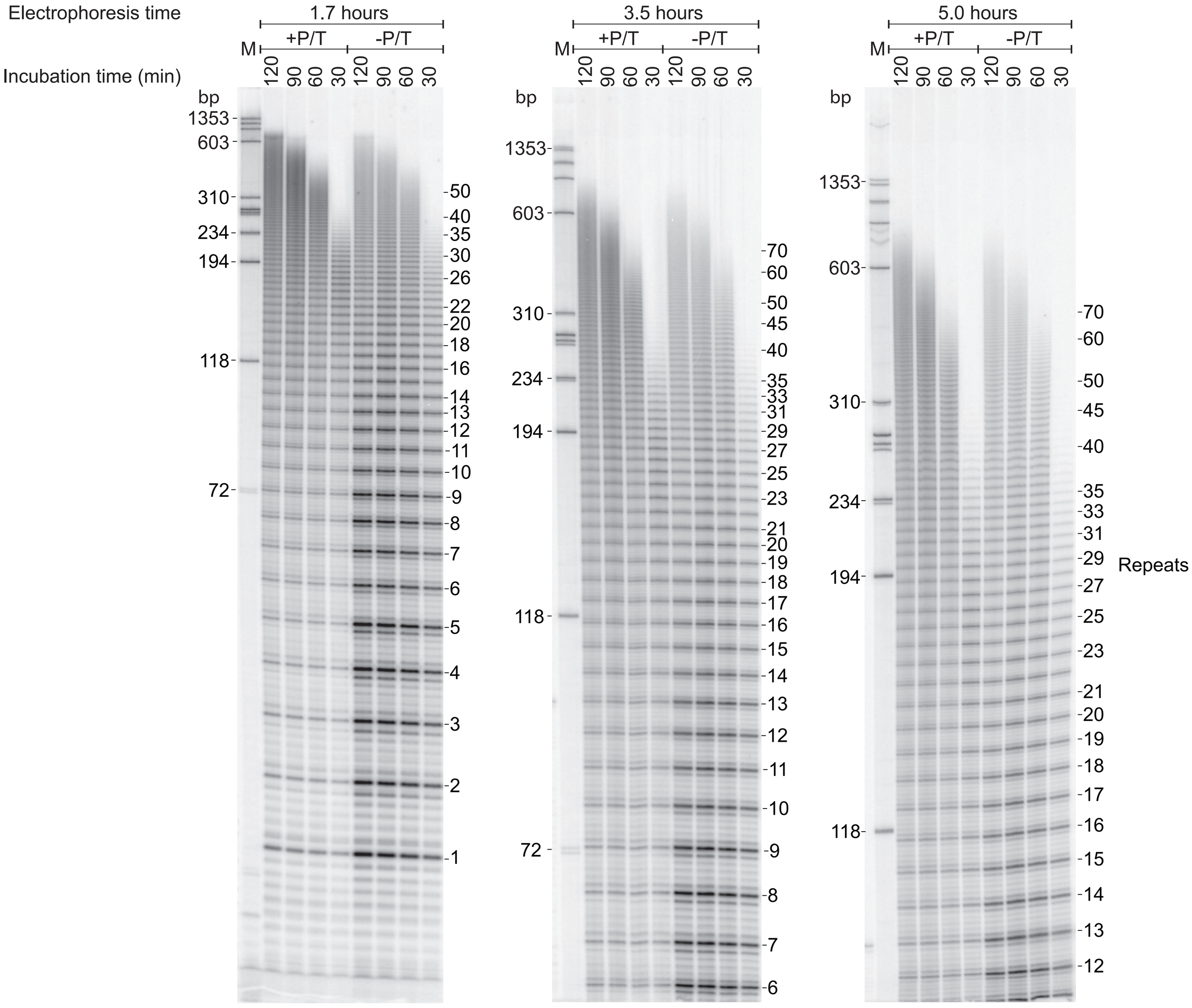

Supplementary Figure S9

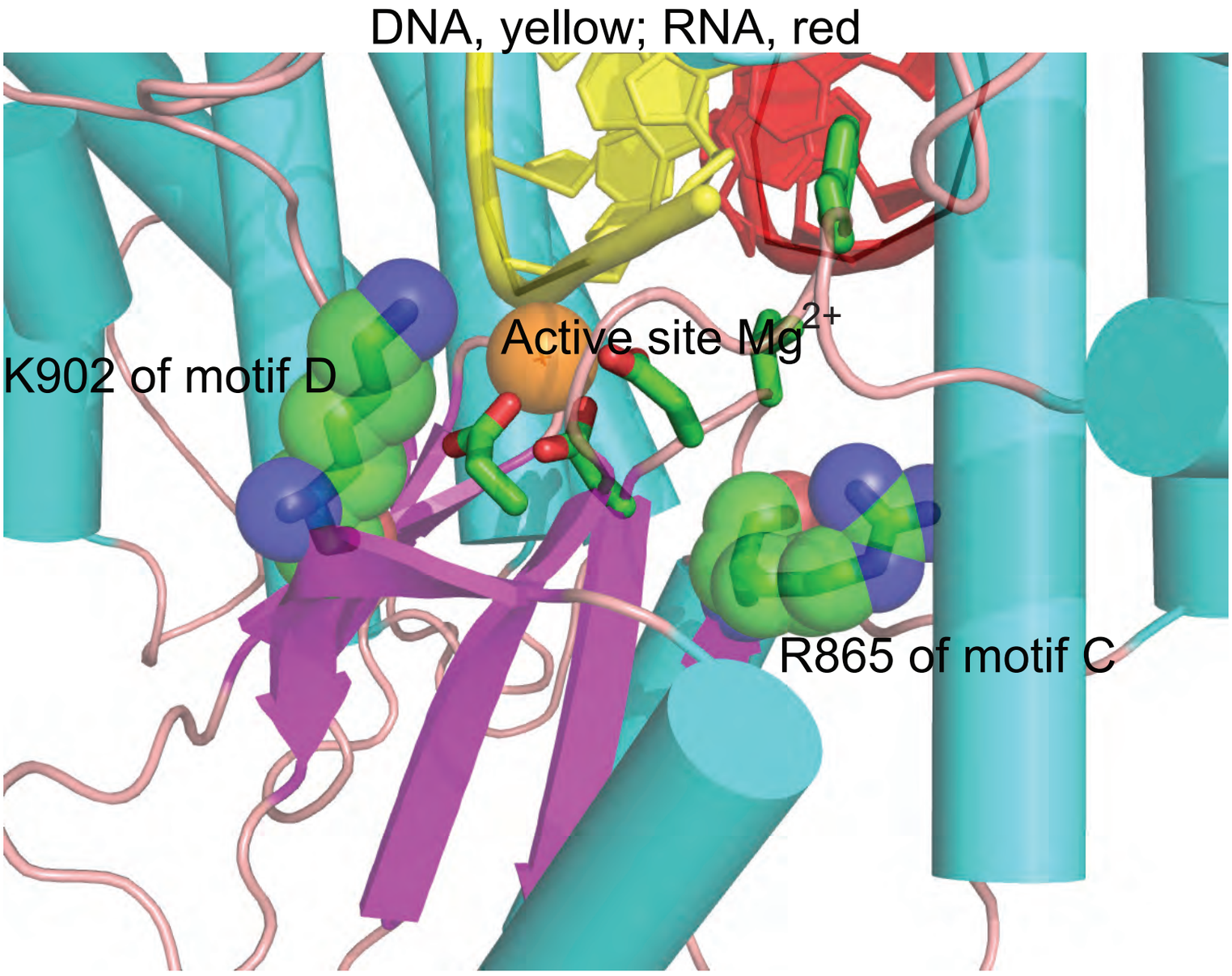

Supplementary Figure S10